American Scientific Research Journal for Engineering, Technology, and Sciences (ASRJETS)

ISSN (Print) 2313-4410, ISSN (Online) 2313-4402

http://asrjetsjournal.org/

The Orthotropic Spline Finite Strip Technique in the Linear Analysis of Ribbed Bridge Decks

Laith Khalid Al-hadithy[a*], Imad Abdulwahid ali[b]

[a]*Asst. Prof. Dr. Civil Engrng. Dpt. /Al-Nahrain University, Baghdad, Iraq*

[b]*State Company for Grain Board, Baghdad, Iraq*

[a]*Email: lthadithy@yahoo.com*

[b]*Email: Emad_aldlyme@yahoo.com*

Abstract

This study presents an efficient simplification on the utility of the spline finite strip method SFSM in the analysis of orthotropic and ribbed bridge decks by conducting two stages of analogy. The actual ribbed bridge deck (practically subjected to combined plate-bending and plane stress actions) is, first, converted into and equivalent orthotropic plate, which is subsequently divided into orthotropic finite strips submitted to plate-bending action only with the use of B_3-spline function to express the displacement function in the longitudinal direction of strips. A programming code using MATLAB computer package is constructed for the analysis of orthotropic plates by the spline finite strip method, where the fewest admissible number of longitudinal sections and local B_3-spline functions has been employed to check its efficiency. When applied to a ribbed RC bridge deck of four transverse diaphragms, the present *orthotropic spline finite strip* technique has proved its reliability in the analysis of such decking system where very high degrees of coincidence of its results with those of the finely meshed sophisticated finite element method attaining 98.4, 86.9 and 95.6 for midspan deflection and longitudinal and transvers bending moments, respectively, have been obtained.

Keywords: Spline Finite Strip Method (SFSM);Geometrical Orthotropy; Ribbed Bridge Decks; Plate-Bending action; B_3-Spline Function.

---

* Corresponding author.

1. Introduction

The analysis of bridge decks can be carried out by several methods. The finite strip method (FSM) is one of those methods. The first use of the finite strip method was in 1968 by Cheung[1] for analysis of rectangular plates with two opposite simply supported ends. In this method the structure is divided into a number of strips by longitudinal lines named *nodal lines*. It is a special form of the finite element method (FEM) where , both methods use the displacement approach, while the (FEM) uses polynomial displacement functions in all directions, the (FSM) uses a simple polynomial in the transverse direction and continuously differential smooth series in the longitudinal (major) direction where their a product together gives the displacement function of the strip.

2. Basic concept and development the spline finite strip method (SFSM)

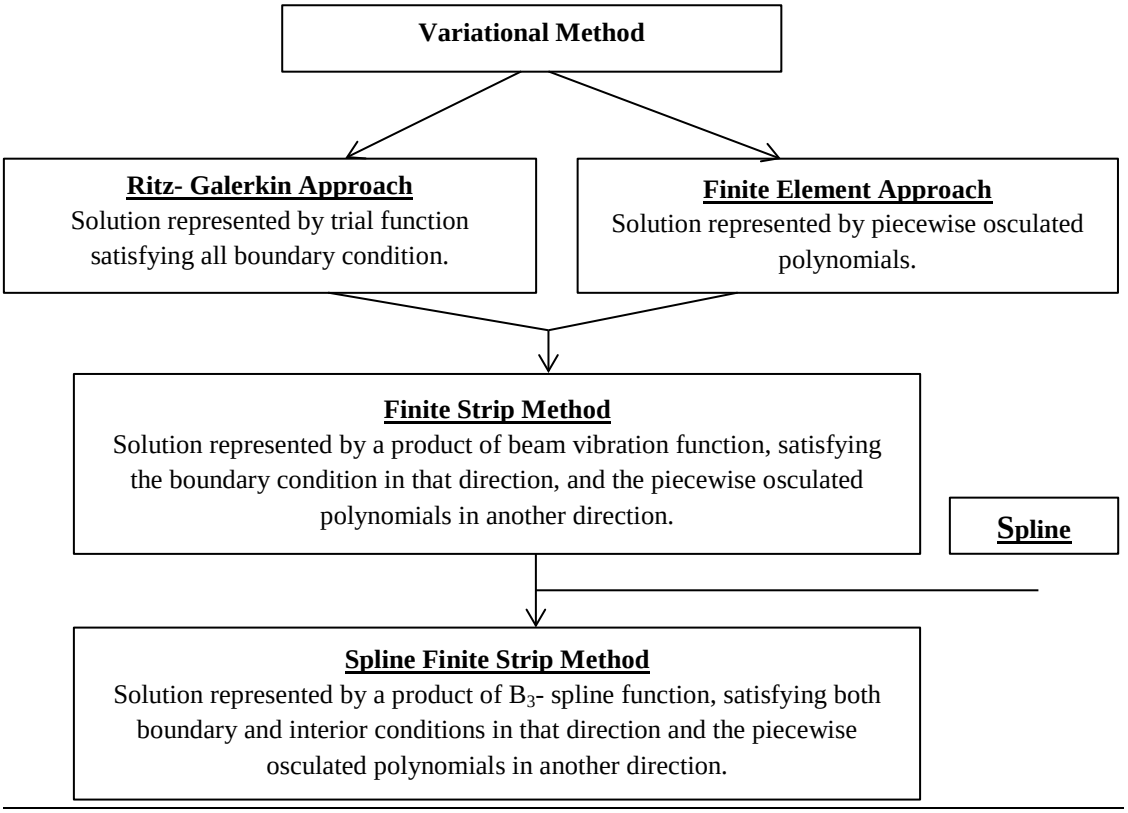

Figure 1: Development and derivation of the basic concept of the spline finite strip method [4]

The conventional finite strip method, introduced by Cheung, depends on using free vibration function series of a beam as a basic function in the longitudinal direction, and osculated polynomials as the interpolation function in the transvers direction [2] The beam vibration function is an infinite series which cannot be obtained by calculation so that numerous numerical experiments must be done to find a suitable and acceptable truncation of the series for all loading cases. Moreover, the infinite continuity of the free vibration functions, hinders its further development, hence the introduction of the highly continuous vibration functions will result in a poor approximation if the series is truncated too early or yielding an oscillated value, when more terms are taken,

Gibb's phenomenon will be valid. On the other hand "the SFSM produces monotonic convergence of stress instead of oscillatory convergence of stress (encountered when using FSM as identified by Gibb's phenomenon) " [3]. This is attributed to the development and structure of the spline finite strip method (SFSM) shown in Figure 1.

3. Displacement function

The longitudinal B_3-spline representation and the transverse interpolation polynomial are multiplied to introduce the displacement function. They are discussed separately

3.1 B_3-Spline representation for longitudinal direction

Several types of splines, were developed in the elapsing century. The most efficient and versatile one is the basic cubic B_3- spline, defined in equation(1) and adopted in this paper.

$$q = \frac{1}{66h^3} \cdot \begin{cases} 0 & , x < x_{i-2} \\ (x - x_{i-2})^3 & , x_{i-2} \le x \le x_{i-1} \\ h^3 + 3h^2(x - x_{i-1}) + 3h(x - x_{i-1})^2 - 3(x - x_{i-1})^3 & , x_{i-1} \le x \le x_i \\ h^3 + 3h^2(x_{i+1} - x) + 3h(x_{i+1} - x)^2 - 3(x_{i+1} - x)^3 , & , x_i \le x \le x_{i+1} \\ (x_{i+2} - x)^3 & , x_{i-1} \le x \le x_i \\ 0 & , x_{i+2} < x \end{cases}$$

……(1)

Derivation of the B_3- spline and the synthesis processes are shown in Figure 2

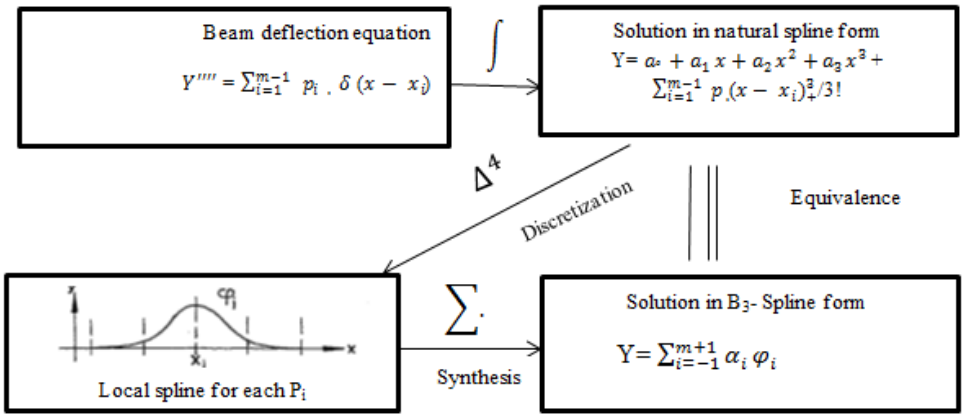

Figure 2: Derivation of B_3-spline expression from natural spline through discretization and synthesis processes

3.1.2 Amendments of boundary conditions

In order to adapt various boundary conditions at end knots, only three boundary local spline centered at each end have to be amended, while the standard B_3-spline, defined by equation (1) is used for other knots.

i.e.

$$Y=[\tilde{\varphi}_{-1}, \tilde{\varphi}_0, \tilde{\varphi}_1, \varphi_2, \varphi_3, \ldots\ldots, \varphi_{m-3}, \varphi_{m-2}, \tilde{\varphi}_{m-1}, \tilde{\varphi}_m, \tilde{\varphi}_{m+1}] \begin{Bmatrix} \alpha_{-1} \\ \alpha_0 \\ \alpha_1 \\ \alpha_2 \\ \alpha_3 \\ \vdots \\ \alpha_{m-3} \\ \alpha_{m-2} \\ \alpha_{m-1} \\ \alpha_m \\ \alpha_{m+1} \end{Bmatrix} \quad \ldots\ldots(2)$$

In short form, $Y = \varphi \,.\, \{\alpha\}$.

Shapes of amended local splines $\tilde{\varphi}_0$ and $\tilde{\varphi}_1$ are shown in the Figure 3

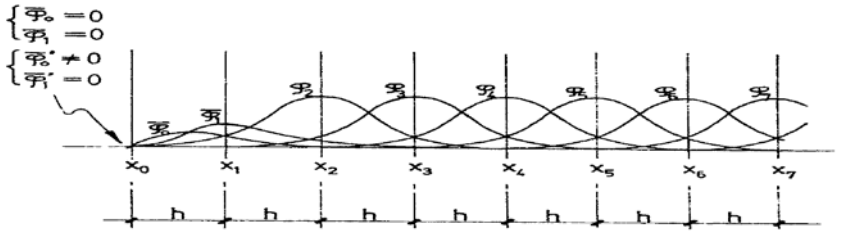

Figure 3: Shapes of amended local splines $\tilde{\varphi}_0$ and $\tilde{\varphi}_1$. [4]

Table 1: Amendment scheme for boundary local splines satisfying both rigid and natural conditions

Amended / Boundary condition		$\tilde{\varphi}_{-1}$	$\tilde{\varphi}_0$	$\tilde{\varphi}_1$
Free End	$y(x_0) \neq 0$ $y'(x_0) \neq 0$ $y''(x_0) = 0$	Eliminated	$\varphi_0+2\varphi_{-1}$	$\varphi_1+\varphi_0+\varphi_{-1}$
Simply Supported End	$y(x_0) \neq 0$ $y'(x_0) \neq 0$ $y''(x_0) = 0$	Eliminated	Eliminated	$\varphi_1- \varphi_{-1}$
Clamped End	$y(x_0) = 0$ $y'(x_0) = 0$ $y''(x_0) \neq 0$	Eliminated	Eliminated	$\varphi_1- \frac{1}{2}\varphi_0+\varphi_{-1}$
Sliding Clamped End	$y(x_0) \neq 0$ $y'(x_0) = 0$ $y(x_0) \neq 0$	Eliminated	φ_0	$\varphi_1+\varphi_{-1}$

3.2 Transverse interpolation polynomials

The transverse interpolation polynomial of two nodal lines of finite strip is used to describe its interior behavior, and it is transformed to the form of shape function [5].

There are many shape functions can obtained by either direct inspection or matrix transformation which are suitable for transverse representation as they satisfy some conditions. The cubic interpolation defining two degrees (the displacement and its derivative) of freedom for each nodal line of a strip is adopted. *The four* appropriate shape functions are:

$$N1 = 1- 3\bar{x}^2 + 2\bar{x}^3 \quad , \quad N2 = x\,(1-2\bar{x} +\bar{x}^2)$$

$$N3 = 3\bar{x}^2 - 2\bar{x}^3 \quad , \quad N4 = x\,(\bar{x}^2 - \bar{x})$$

where $\bar{x} = \frac{x}{b}$

These shape functions, are derived from a straight line connecting two nodes, with displacement and transverse rotation as shown in Figure 4, they are derived with their derivatives by direct inspection.

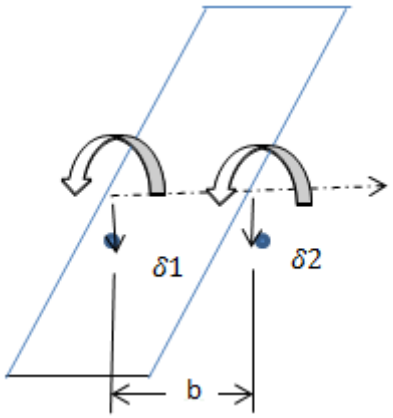

Figure 4: Transverse shape function in connection with the degrees of freedom of two edge nodal lines.

4. Formulation of the strip characteristics

After choosing the displacement function for describing the behavior of the strip element, the analysis can then proceed simply by following the standard procedures for discrete systems using displacement approach. The strip characteristics including stiffness matrix, load matrix and mass matrix can then obtained by variational method or its equivalence- the principle of minimum total potential energy. The basic procedures are as following:

- Choose a suitable displacement function **[f]** for all defined degrees of freedom.
- Construct the strain matrix **[B]** according to the kinematic relationship between strains $\{\varepsilon\}$and displacement parameters **$\{\delta\}$**

i.e. $\{\varepsilon\} = [B]\ \{\delta\}$ …..(3)

- Connect the stress $\{\sigma\}$ to the displacement parameters $\{\delta\}$ through constitutive equation

$$\{\sigma\} = [D]\ \{\varepsilon\} \quad \text{…..(4)}$$

In which **[D]** is the property matrix. Hence

$$\{\sigma\} = [D]\ [B]\ \{\delta\} \quad \text{…..(5)}$$

- Drive the stiffness matrix and load matrix through the principle of minimum total potential energy. The potential energy consist of two parts:

(i) Strain energy stored in the strips of volume V

i.e. $\pi_1 = \frac{1}{2}\int_V \{\varepsilon\}^T . \{\sigma\}\, dv$

$$= \frac{1}{2}\int_V \{\delta\}^T . [B]^T [D] [B] \{\delta\} dv \quad \text{…..(6)}$$

(ii) Potential energy of the applied loads q_i over area A_i respectively.

i.e. $\pi_2 = -\sum_i \int_{Ai} \{f\}^T . q_i\, dA_i$

$$= -\sum_i \int_{Ai} \{\delta\}^T [\Phi]^T [N]^T . q_i\, dA_i \quad \text{…..(7)}$$

Hence, the total potential energy of the system is

$$\pi = \pi_1 + \pi_2$$

$$= \frac{1}{2}\int_V \{\delta\}^T . [B]^T [D] [B] \{\delta\} dv - \sum_i \int_{Ai} \{\delta\}^T [\Phi]^T [N]^T . q_i\, dA_i \quad \text{…..(8)}$$

It depends on the variables $\{\delta\}$ only.

By taking first variation, $\partial\pi = 0$, it gives

$$\left[\int_V [B]^T [D] [B]\, dv\right] \{\delta\} = \sum_i \int_{Ai} [\Phi]^T [N]^T\ q_i\, dA_i \quad \text{…..(9)}$$

In short form,

$$[K] . \{\delta\} = \{f\} \quad \text{…..(10)}$$

- Carry out the integrations over the whole volume of each strip or the loaded area and use the following

expressions to obtain the stiffness matrix $[K]_e$, mass matrix $[M]_e$ and the load matrix $\{f\}_e$ respectively.

i.e. $$[K]_e = \int_V [B]^T [D] [B] \, dv \quad \text{.....(11)}$$

5. Analysis of thin rectangular plates in bending by spline finite strip method (SFSM)

The behavior of a strip in the spline finite strip analysis is described by its two boundary nodal lines. So, the prescribed conditions have been incorporated into the B_3-Spline expression for the nodal lines, hence, there will be no difference in solution procedures for different boundary or interior conditions. The solution presented here is based on Kirchhoff's theory**,** which enables the problem of thin plate bending to be treated as a two-dimensional one.

5.1 Degrees of freedom

Two degree of freedom for each nodal line (according to the convergence criteria) are necessary to acquire the minimum compatibility conditions. i.e. the lateral displacement, **w**, and the first derivative, $\boldsymbol{\theta}_{xz} = \frac{\partial_w}{\partial_x}$ with respect to the transverse x-axis, as shown in Figure 5.

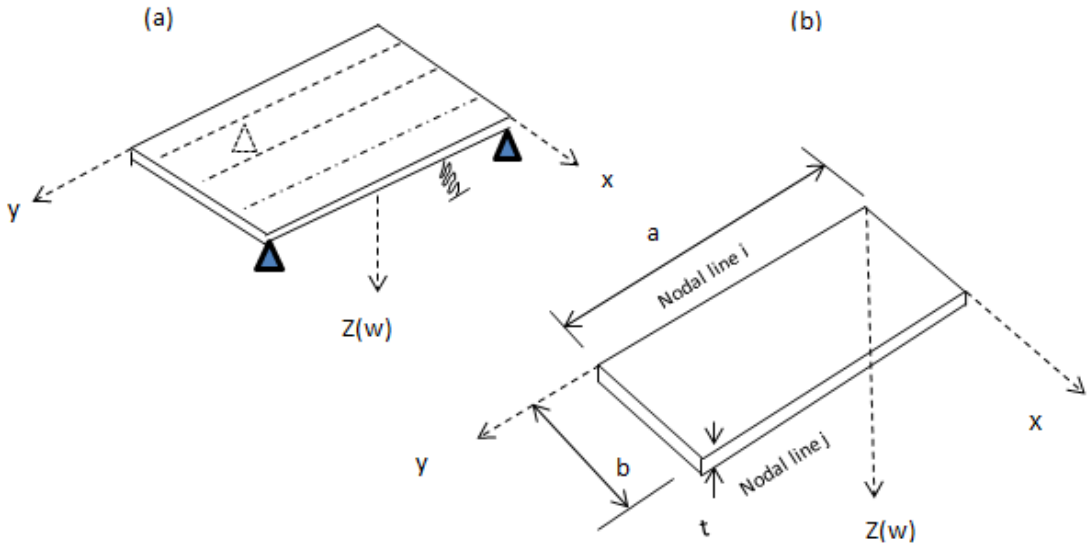

Figure 5: Rectangular plate strip analysis. (a) Plate as an assembly of strips; (b) Typical strip

5.2 Stiffness matrices

The stiffness matrix [**k**] can be worked manually and expressed in explicit form, after deriving the displacement function and the expressions of relationships between the strain– displacement and the stress–strain. Finally Table 2 is got.

where:

$$\begin{cases} \mathbf{D}_x = \frac{\mathbf{E_x} \cdot \mathbf{t}^3}{12(1-\mathbf{v_x v_y})} \\ \mathbf{D}_y = \frac{\mathbf{E_y} \cdot \mathbf{t}^3}{12(1-\mathbf{v_x v_y})} \\ \mathbf{D_1} = \boldsymbol{v_x} \cdot \mathbf{D}_y = \boldsymbol{v_y} \cdot \mathbf{D}_x \\ \mathbf{D}_{xy} = \frac{\boldsymbol{G_{xy}} \cdot \boldsymbol{t}^3}{12} \end{cases} \quad \ldots\ldots(12)$$

and, $\mathbf{E_x}$, $\mathbf{E_y}$ are Young's moduli, v_x , v_y are Poisson's ratios,

and $\boldsymbol{G_{xy}}$ is shear modulus = $\frac{\sqrt{E_x^{elem} E_y^{elem}}}{2(1+\sqrt{v_x v_y})}$ [6]

Poisson's ratio in the y direction v_y May be considered as:

$$(\boldsymbol{v_y} = \boldsymbol{v_x} \frac{E_y}{E_x}) \qquad [7]$$

Table 2: Bending stiffness matrix of a rectangular strip [4]

$[K] = \frac{1}{420b^3}$

5040		D_x	$I_{1_{11}}$	2520	b	D_x	$I_{1_{12}}$	-5040		D_x	$I_{1_{13}}$	2520	b	D_x	$I_{1_{14}}$
-504	b^2	D_1	$I_{2_{11}}$	-462	b^3	D_1	$I_{2_{12}}$	+504	b^2	D_1	$I_{2_{13}}$	-42	b^3	D_1	$I_{2_{14}}$
-504	b^2	D_1	$I_{3_{11}}$	-42	b^3	D_1	$I_{3_{12}}$	+504	b^2	D_1	$I_{3_{13}}$	-42	b^3	D_1	$I_{3_{14}}$
+156	b^4	D_y	$I_{4_{11}}$	+22	b^5	D_y	$I_{4_{12}}$	+54	b^4	D_y	$I_{4_{13}}$	-13	b^5	D_y	$I_{4_{14}}$
+2016	b^2	D_{xy}	$I_{5_{11}}$	+168	b^3	D_{xy}	$I_{5_{12}}$	-2016	b^2	D_{xy}	$I_{5_{13}}$	+168	b^3	D_{xy}	$I_{5_{14}}$
				1680	b^2	D_x	$I_{1_{22}}$	-2520	b	D_x	$I_{1_{23}}$	840	b^2	D_x	$I_{1_{24}}$
				-56	b^4	D_1	$I_{2_{22}}$	+42	b^3	D_1	$I_{2_{23}}$	+14	b^4	D_1	$I_{2_{24}}$
				-56	b^4	D_1	$I_{3_{22}}$	+42	b^3	D_1	$I_{3_{23}}$	+14	b^4	D_1	$I_{3_{24}}$
				+4	b^6	D_y	$I_{4_{22}}$	+13	b^5	D_y	$I_{4_{23}}$	-3	b^6	D_y	$I_{4_{24}}$
				+224	b^4	D_{xy}	$I_{5_{22}}$	-168	b^3	D_{xy}	$I_{5_{23}}$	-56	b^4	D_{xy}	$I_{5_{24}}$
								5040		D_x	$I_{1_{33}}$	-			
								-504	b^2	D_1	$I_{2_{33}}$	2520	b	D_x	$I_{1_{34}}$
								-504	b^2	D_1	$I_{3_{33}}$	+462	b^3	D_1	$I_{2_{34}}$
								+156	b^4	D_y	$I_{4_{33}}$	+42	b^3	D_1	$I_{3_{34}}$
								+2016	b^2	D_{xy}	$I_{5_{33}}$	-22	b^5	D_y	$I_{4_{34}}$
												-168	b^3	D_{xy}	$I_{5_{34}}$
												1680	b^2	D_x	$I_{1_{44}}$
												-56	b^4	D_1	$I_{2_{44}}$
												-56	b^4	D_1	$I_{3_{44}}$
												+4	b^6	D_y	$I_{4_{44}}$
												+224	b^4	D_{xy}	$I_{5_{44}}$

Where:

$I_{1_{ij}} = \int_0^a \varphi^{T}{}_i \varphi_j d_y$;

$I_{2_{ij}} = \int_0^a \varphi^{"T}{}_i \varphi_j d_y$;

$I_{3_{ij}} = \int_0^a \varphi^{T}{}_i \varphi^{"}{}_j d_y$;

$I_{4_{ij}} = \int_0^a \varphi^{"T}{}_i \varphi^{"}{}_j d_y$;

$I_{5_{ij}} = \int_0^a \varphi'^{T}{}_i \varphi'{}_j d_y$.

Symmetry

5.3 Load matrices

(i) For a patch load linearly distributed along y- direction from y_1 to y_2 (Figure 6): The load vector {F} can be

expressed as:

$$\{F\} = \int_0^b \int_{y1}^{y2} [\varphi]^T [N]^T \{ q_1 + (\frac{q_2 - q_1}{y_2 - y_1}) (y - y_1) \} d_x d_y \quad \ldots\ldots(13)$$

$$\{F\} = q_1 (\int_{y1}^{y2} [\varphi]^T d_y . \begin{Bmatrix} b/2 \\ b^2/12 \\ b/2 \\ -b^2/12 \end{Bmatrix} + (\frac{q_2 - q_1}{y_2 - y_1}) (\int_{y1}^{y2} [\varphi]^T (y - y_1) d_y) \begin{Bmatrix} b/2 \\ b^2/12 \\ b/2 \\ -b^2/12 \end{Bmatrix} \quad \ldots\ldots(14)$$

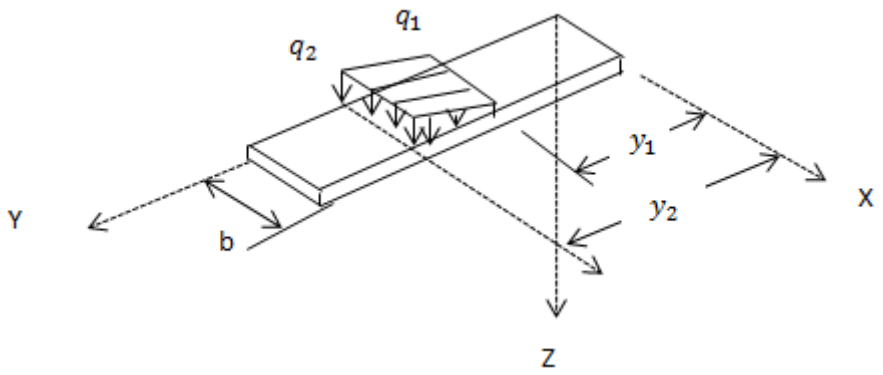

Figure 6: Linearly distributed patch load on a rectangular plate strip

(ii) For a concentrated load on a nodal line:

To get more accuracy it is recommended to locate a nodal line passing through the concentrated load, otherwise its effect can only be transferred to its two boundary nodal lines through the cubic interpolation polynomial of the assumed displacement function. With reference to Figure 7 the comprehensive load vector for the combination of a concentrated load **P**, moment $\mathbf{m}_x$ and moment $\mathbf{m}_y$ at locations $\mathbf{y_1}, \mathbf{y_2}, \mathbf{y_3}$ on nodal line **i**, respectively, is expressed in matrix form as follows:

$$\{F\} = [\varphi(y_1)]^T \begin{Bmatrix} P \\ 0 \\ 0 \\ 0 \end{Bmatrix} + [\varphi(y_2)]^T \begin{Bmatrix} 0 \\ M_x \\ 0 \\ 0 \end{Bmatrix} + [\varphi'(y_3)]^T \begin{Bmatrix} M_y \\ 0 \\ 0 \\ 0 \end{Bmatrix} \quad \ldots\ldots(15)$$

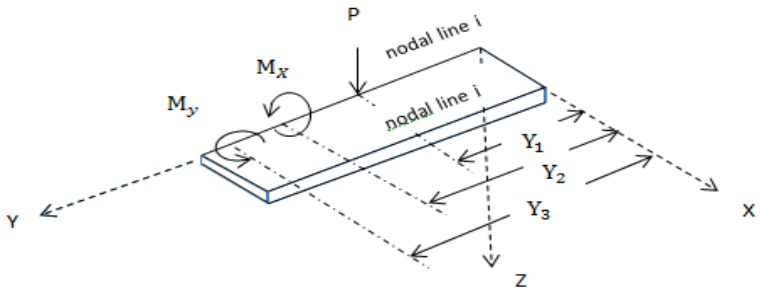

Figure 7: Concentrated loads on nodal line of rectangular plate strip.

In Eq. 15 each of the three components forms a column vector with four non-zero entries only, since there are only four local splines contributing non-zero values to it at the specified location y_i , as shown in Figure 8.

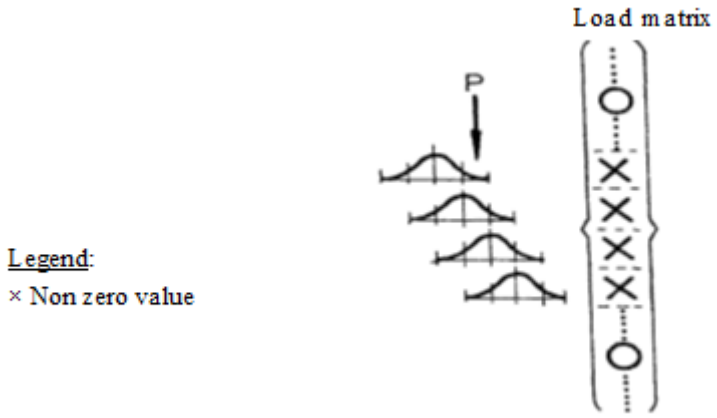

Figure 8: Local splines associated with concentrated load p and their contributions to load matrix.

(iii) For uniform distribution load q [8]

$$\{F\} = \int_0^a \int_0^b q\,[\varphi]^T\,[N]^T\,dx\,dy$$

$$= q\int_0^a [\varphi]^T\,dy \cdot \int_0^b [N]^T dx = q\int_0^a [\varphi]^T\,dy \cdot \begin{Bmatrix} b/2 \\ b^2/12 \\ b/2 \\ -b^2/12 \end{Bmatrix} \qquad \ldots\ldots(16)$$

6. Orthotropic plate analogy

The term " *Orthotropic Plate*" explicitly refers to plates of either material or geometrical orthotropy. "A *materially orthotropic*" plate is composed of a homogeneous material which has different elastic properties in two orthogonal directions but the same geometric properties**",[Eugene,2005]**[2] ,i.e. the plate has the same second moment of area in both orthogonal principal directions but with different moduli of elasticity. It should be noted that such a slab(materially orthotropic plate) is not found in bridge decks, it is an accurate approximation of some practical condition like timber. Most bridge decks slabs have different values of the second moment of area in the two orthogonal principal directions, such as voided slabs, and reinforced concrete ones(since different amounts of reinforcement are used in those two directions), such types of slabs are referred to as *geometrically orthotropic* [6,10]

7. Procedure of the present analysis of ribbed bridge decks

The present analysis consist of two discrete stages; a preparatory stage (previously treated by researchers in the field of deck simulation), and the major stage concerning orthotropic SFSM analysis *solely treated by the present work.*

7.1 First (preparatory) stage: Modeling the ribbed bridge deck by equivalent materially orthotropic plate

This stage is summarized in the following steps:-

1- Calculating the second moments of area per unit width (or length) of the deck cross-sections in both orthogonal directions of the deck (I_x and I_y, respectively).

2- Finding the new equivalent thickness by using Equation 17, which means getting the equivalent orthotropic plate (solid plate) that has a constant thickness ($I_x = I_y$).

$$d = \sqrt[3]{12I} \qquad \text{.....(17)}$$

3- Calculation of the new modulus of elasticity $\mathbf{E_y}$ and Poisson's ratio $\boldsymbol{\nu_y}$ in the transverse (**y**) direction, using Eqs. 18 and 19, respectively.

$$E_y^{elem} = E^{slab}\frac{I_y^{slab}}{I_x^{slab}} \qquad \text{.....(18)}$$

$$\nu_y = \nu_x\frac{E_x}{E_y} \qquad \text{.....(19)}$$

4- Finding the equivalent rigidities of the equivalent materially orthotropic plate, which is found by using Eq.12. This technique is schematically shown in Figure 9 .

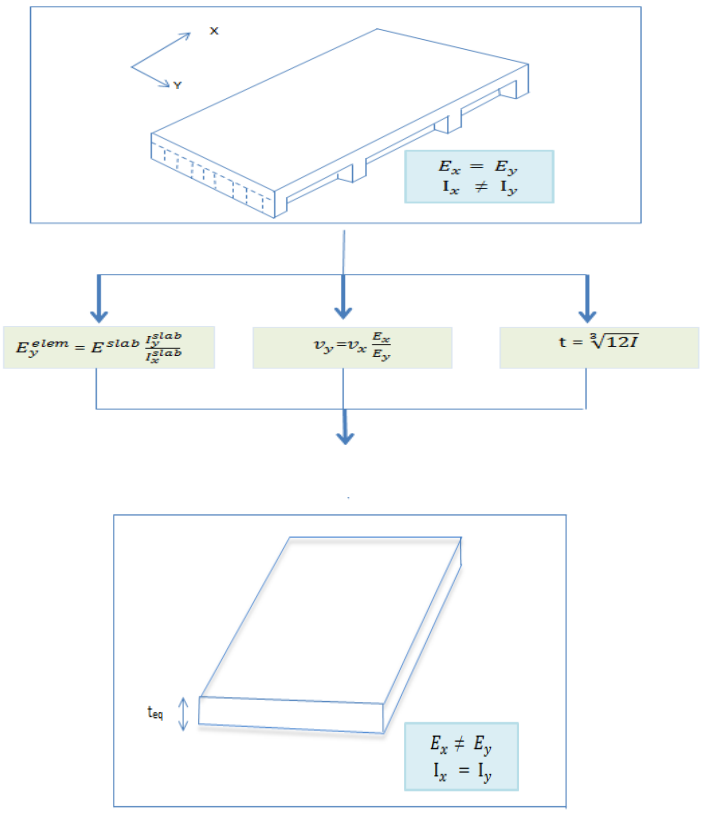

Figure 9: Materially orthotropic plate technique.

7.2 The second (main) stage

The analysis of equivalent orthotropic plates by using the B_3-spline finite strip method under bending action in this study is formulated by MATLAB computer package where a programming code named RAOBDB3SFSM has been constructed. Formulation of the program consists of two stages :-

A- ***<u>Stage I</u>***

This stage involves formulation of the bending stiffness matrix of a rectangular strip according to the following steps:

1. Calculating values of the coupling integrations represented by $I_{1_{ij}}$, $I_{2_{ij}}$, $I_{3_{ij}}$, $I_{4_{ij}}$ and $I_{5_{ij}}$.
2. Formulation of the submatrices:

The dimensions of each (4x4) bending stiffness submatrix, previously determined and given in Table 3,will be according to the number of sections into which the nodal line has been discretized. In the present work a fixed number of equally spaced sections (five equally spaced sections; m=5) has been adopted. Hence, the dimensions of each submatrix will be (m+3) × (m+3) = [8x8], therefore the dimensions of each rectangular strip will be 32x32 .

3. Formulating the global stiffness matrix:

The global stiffness matrix dimensions will be according to the number of strips to which the plate was divided. Primary four strips will be taken, so dimensions of the global stiffness matrix will become 80 x 80 .

B- ***<u>Stage II</u>***

This stage involves formulation of the load matrices by the following steps:

1- According to the cases of load which are explained previously, the integration of each local B_3-spline function (hill) along the nodal line will be carried out, where each nodal line contains 8 hills; φ_{-1}, φ_0, ... , φ_6 .This function integration is also performed utilizing the facilities of MATLAB program.
2- The B_3- spline is considered to be amended with the aid of table 2.
3- Combination of all the integration values common to each knot.
4- Constructing the [**10x80**] load vector {F}, for each of the four strips.
5- The unknown displacement parameters are carried out by solving the equation:

$$\{F\} = [K] \,.\, \{\delta\}$$

using the Gauss elimination procedure.

8. Application: Full scale R.C. slab-beam ridge Deck (seven ribs +four diaphragms)

8.1 Description

This case is represented by a simply supported reinforced concrete slab-beam bridge deck, with seven ribs and four diaphragms as shown in Figure 10. The bridge is under a central 150 kN vertical concentrated load.

Geometrical features and material properties are as follows:

Span × Width	= 25000×15000	mm
Slab thickness	= 200	mm
28- day compressive strength; f_c'	= 30	N/mm^2
Modulus of elasticity	= 28	kN/mm^2
Poisson's ratio	= 0.15	

These values are in compliance with BS 5400

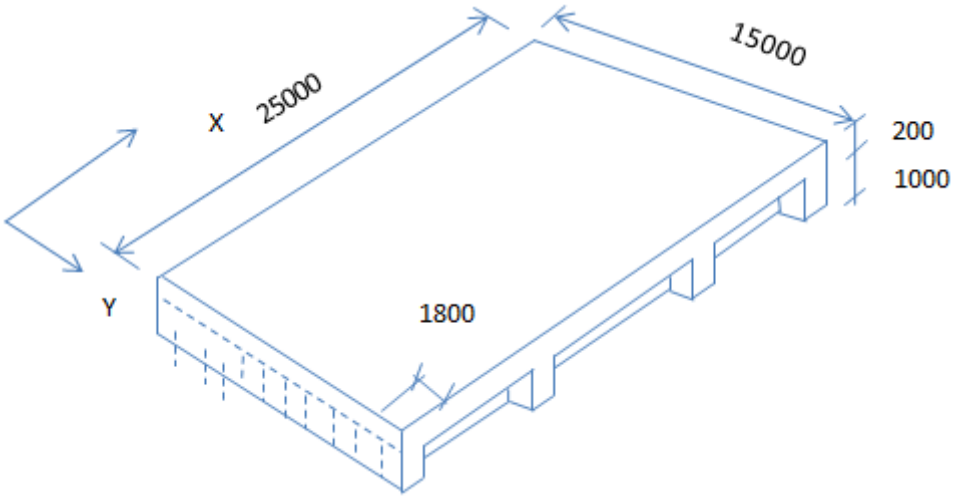

Figure 10: Reinforced concrete slab-beam bridge deck with seven ribs and four diaphragm**.**

8.2 Analysis methods

Rigidities of the substitute orthotropic plate have been computed as previously instructed in this paper, they are given in Table 3 below.

Table 3: Rigidities of the slab-beam bridge deck of seven ribs and four diaphragms.

Flexural rigidities	D_x	1079239551	kN.mm
	D_y	201570929	kN.mm
Torsional rigidity	D_{xy}	299573891	kN.mm
Coupling rigidity	D_1	11287972	kN.mm

According to the new technique explained in the elapsing section, the equivalent elastic properties of the substitute orthotropic plate are: t_{eq} =478mm , E_x = 74.96 kN.mm, υ_x = 0.4

and considering that $D_1 = \upsilon \times$ (the smallest value of D_x or D_y).

This ribbed bridge deck was previously analyzed by Mehdi [11] using the grillage analogy.

8.3 Analysis results

Values of deflection computed by three methods of analysis are given in Tables 4 and 5, then shown in figure11 below.

Table 4: Deflection values (in mm) of R.C ribbed bridge deck

x-coordinate(mm)	-12500	-7500	-2500	0	2500	7500	12500
SFSM(present study) No. of strip=4 No. of section=5	0	1.85	2.96	3.10	2.95	1.85	0
FEM (**SAP2000**) (*15x25 meshes*)	0	1.73	2.95	3.15	2.95	1.73	0
Grillage analysis **Mehdi [11]**				3.21			

Table 5: Comparison of maximum moments M_x and M_y (in kN.mm/mm) of the R.C bridge deck.

Method of analysis	Mx (kN.mm/mm)	My (kN.mm/mm)
Present SFSM	41.17	21.25
FEM (**SAP2000**) (*15x25 meshes*)	47.37	20.36

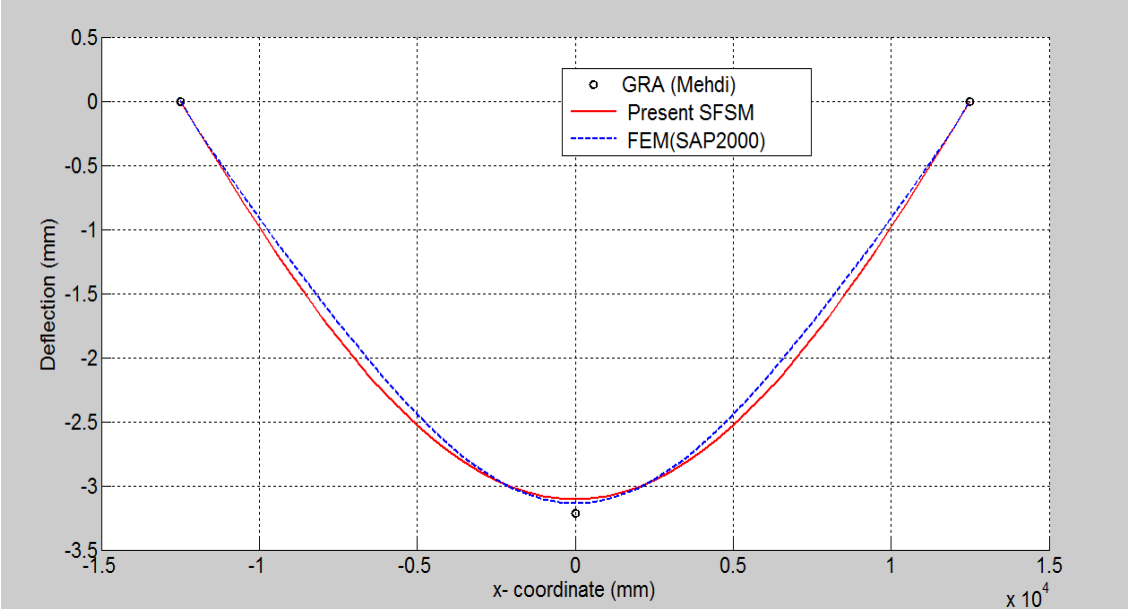

Figure 11: Variation of deflection along x-centerline of the R.C. ribbed bridge deck.

8.4 Discussion of analysis results

a) Agreement of deflection results

i) Inspection of Table 4 which gives deflection values by the three methods of analysis, high agreements between values obtained by the present SFSM (in its least number of strips and sections) and those obtained by the other methods -especially the finite element method FEM implemented by SAP2000 rather fine mesh- .

ii) The percentage differences of the maximum deflection value, as shown in the bar chart of Figure 12 is 1.6 % .

iii) Observing Figure 11 which concerns spanwise variations of deflection along centerlines of the bridge deck, quite close variation curves are produced which definitely indicate the high accuracy and efficiency of the present SFSM treatment of ribbed bridge decks by the equivalent orthotropic plate

replacement.

b) Agreement of bending moment results

i) Referring to Table 5 specialized in comparative bending moment values computed by the two method analysis (with utilizing the finite difference technique, obviously good agreements between values produced by the present SFSM and FEM (SAP2000) (in spite of incorporation of the approximate finite difference technique) .

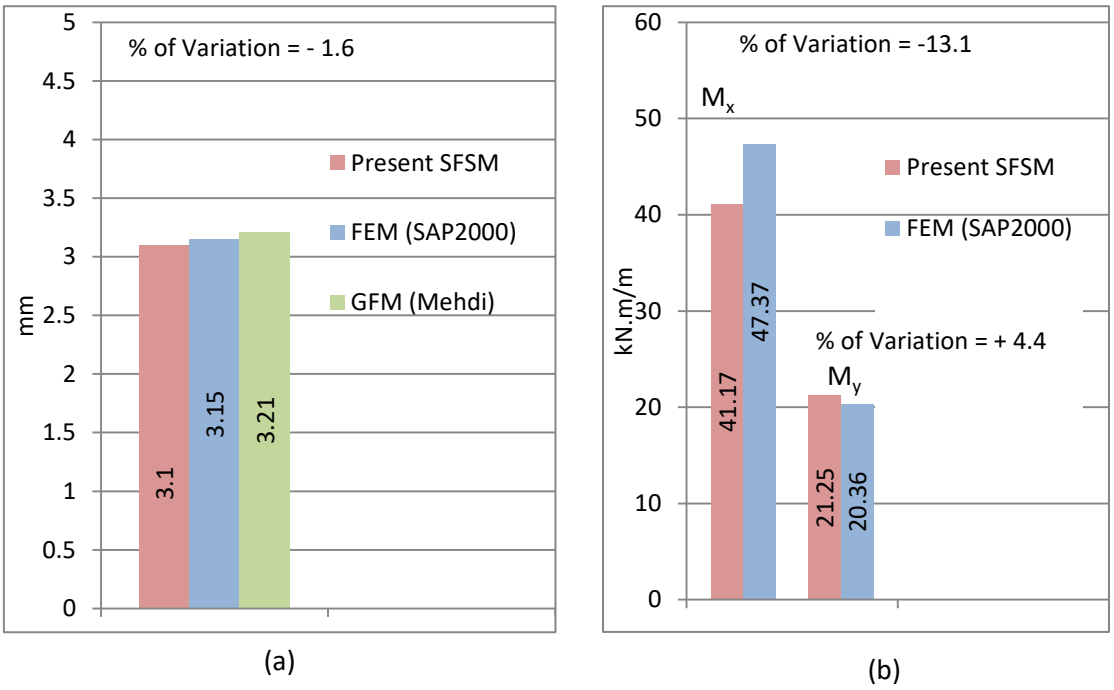

Figure 12: Comparative chart showing values of : (a) The max. deflection, (b) The max. moment at centerline of bridge deck.

9. Conclusions

Based on the results of the present SFSM analysis the following conclusions have been drawn so far:

1. The use of spline finite strip method (SFSM) in the analysis of ribbed bridge decks by initially treating them as equivalent orthotropic plates has just been proved to be simpler, faster, more feasible and more economical than the finite element method. Meanwhile, it is more accurate and more versatile than the grid framework analogy.
2. Proposing a new technique for analysis orthotropic plates based on converting the section of geometrical orthotropic plate to equivalent section of materially orthotropic plate using simplified expressions for elastic rigidities in that purpose has proved to be efficient and reliable
3. In the analysis of ribbed bridge decks more accuracy can be obtained when the equivalent thicknesses in the two orthogonal directions(i.e. t_x and t_y) of such plates are calculated twice, first by taking the

thickness obtained from the equation ($t_x = \sqrt[3]{12I_x}$), and second by taking the thickness obtained from the equation ($t_y = \sqrt[3]{12I_y}$) . Consequently, deflection values are obtained by averaging its two different values calculated from two different plate thicknesses.

4. Based on its results of analysis of the full scale reinforced concrete slab-beam bridge deck has four transvers diaphragms, the present SFSM has also revealed extremely high degrees of accuracy for deflection, where the gained levels of coincidence of the present SFSM with the finely meshed SAP2000 model is 98.4%.
5. High levels of coincidence for the results of bending moment M_x and M_y outputs from the present SFSM and finely meshed SAP2000 model for the full scale reinforced concrete slab-beam bridge deck has four transvers diaphragms full scale RC slab-beam bridge deck, where 86.9% and 95.6%, respectively.

10. Recommendation

- The proposed *"Orthotropic Spline Finite Strip*" technique used in the present study for the analysis of ribbed bridge deck can be extended to study other types of bridge deck such as waffle slab decks , voided slab decks, cellular deck slab and box girder bridge decks
- More investigation is needed on the least number of finite strips and /or sections per nodal line giving satisfactory accuracy with a minimum effort of input data preparation and execution time for analysis of ribbed bridge decks by the present orthotropic SFSM

- Investigation on the efficiency of the present orthotropic SFSM in analyzing ribbed bridge decks of varying ribs depth.

References

[1] Cheung, Y.K. "The Finite Strip Method in the Analysis of Elastic Plates with Two Opposite Simply Supported Ends". Proc. Inst. Civ. Engr, Vol. 40, No.7, pp.1-7,1968.

[2] Cheung, M.S., Li, W. and Chidiac, S.E. Finite Strip Analysis of Bridges Bridges. First Edition. London: E&FN Spon,1996.

[3] Razzaq, Raja. javed. "Nonlinear Static and Dynamic Analysis of Composite, Layered plates and shells using Finite Strip methods". Ph. D. Thesis, Granfield university,2003.

[4] Cheong, F.S. "Spline Finite Strip in Structural Analysis". Ph. D. Thesis, University of Hong-Kong,1982.

[5] Cheung, Y. K. Finite Strip Method in Structural Analysis. First edition. : pergamon press,1976.

[6] Eugene J. O'Brien and Damien L. Keogh. Bridge Deck Analysis . first edition. Ireland: E&FN Spoon,2005.

[7] Emran, Amir Habeeb "Experimental and Analytical Study on Orthotropic Plate Theory in Bridge Deck Analysis". M. Sc. Thesis, University of Baghdad,1983.

[8] Cheung, Y.K., and tham, L.G. Finite Strip Method. fourth edition.UK: CRC Press,1997.

[9] Logan, Daryl. L. A First Course in the Finite Element Method. 4th Ed. University of Wisconsin–

Platteville: Thomson,2010.

[10] Al-Hadithy, Laith "Analysis of Indeterminate Bridges by the Orthotropic Plate Theory with Experimental Study". M. Sc. Thesis, University of Baghdad,1985.

[11] Mehdi, Wafa Sadiq "Elastic Analysis of Reinforced Concrete Multiple T- Section Bridge Decks by the Grillage Methods". M. sc. Thesis, University of Technology- Baghdad,1996.

[12] AL-Safarjalani, Modar Tawfik ."Analysis of Skew Plates by the Spline Finite Strip Method". M. Sc. Thesis, University of Baghdad,1988.

[13] Al-Dawar, Mohammed.A.AL-Khaliq ."A Study on the Use of Orthotropic Plate Theory in Bridge Deck Analysis". Ph. D. Thesis, University of Baghdad,1998.

[14] Hassan, Rafea Flaih ."Bridge Deck Analysis using Orthotropic Plate Theory". M. Sc. Thesis, University of Technology- Baghdad,2005.

[15] A.Kadir, Benan Naji. "Analysis of Simply Supported Concrete Highway Bridges using the Orthotropic Plate Theory and Iraqi Specifications". M. sc. Thesis, University of Baghdad,1979.

[16] Timoshenko, S.P. and Kreiger, S.W. Theory of Plate and Shells. 2edEd. New Yourk: McGraw-Hill, 1959.

[17] Cusens, A. R. and Pama, R.P. Bridge Deck Analysis. London: John Wile and Sons, 1975.